JOURNAL OF VIROLOGY, July 2002, p. 6974–6986 Vol. 76, No. 14
0022-538X/02/$04.00+0 DOI: 10.1128/JVI.76.14.6974–6986.2002

Cell Surface Major Histocompatibility Complex Class II Proteins Are Regulated by the Products of the $\gamma_1$34.5 and U_L41 Genes of Herpes Simplex Virus 1

Joanne Trgovcich,[1] David Johnson,[2] and Bernard Roizman[1]*

The Marjorie B. Kovler Viral Oncology Laboratories, The University of Chicago, Chicago, Illinois 60637,[1] and Department of Molecular Microbiology and Immunology, Oregon Health Sciences University, Portland, Oregon 97201[2]

Received 25 January 2002/Accepted 18 April 2002

Modulation of host immune responses has emerged as a common strategy employed by herpesviruses both to establish life-long infections and to affect recovery from infection. Herpes simplex virus 1 (HSV-1) blocks the major histocompatibility complex (MHC) class I antigen presentation pathway by inhibiting peptide transport into the endoplasmic reticulum. The interaction of viral gene products with the MHC class II pathway, however, has not been thoroughly investigated, although $CD4^+$ T cells play an important role in human recovery from infection. We have investigated the stability, distribution, and state of MHC class II proteins in glioblastoma cells infected with wild-type HSV-1 or mutants lacking specific genes. We report the following findings. (i) Wild-type virus infection caused a decrease in the accumulation of class II protein on the surface of cells and a decrease in the endocytosis of lucifer yellow or dextran conjugated to fluorescein isothiocyanate but no decrease in the total amount of MHC class II proteins relative to the levels seen in mock-infected cells. (ii) Although the total amount of MHC class II protein remained unchanged, the amounts of cell surface MHC class II proteins were higher in cells infected with the U_L41-negative mutant, which lacks the virion host shutoff protein, and especially high in cells infected with the $\gamma_1$34.5-negative mutant. We conclude that infected cells attempt to respond to infection by increased acquisition of antigens and transport of MHC class II proteins to the cell surface and that these responses are blocked in part by the virion host shutoff protein encoded by the U_L41 gene and in large measure by the direct or indirect action of the infected cell protein 34.5, the product of the $\gamma_1$34.5 gene.

Herpes simplex virus 1 (HSV-1) has evolved numerous mechanisms to evade or counteract innate and specific host immune responses (reviewed in references 23, 28, and 51). These strategies promote escape from phagocytes, complement, NK cells, and cytotoxic T cells (CTL). In particular, CTL have been shown to be crucial for control of both productive and latent virus infections, and this is mirrored in the plethora of mechanisms which members of the *Herpesviridae* family have adopted to evade major histocompatibility complex (MHC) class I-mediated immune responses (39). HSV-1 and HSV-2 encode at least one protein, the infected cell protein (ICP) 47, which is dedicated to the evasion of CTL-mediated responses to infection (53). ICP47 disrupts normal peptide loading of MHC class I molecules by disabling peptide transport mediated by TAP1/TAP2 (13, 19). However, the extent to which HSV-1 can interfere directly with the MHC class II antigen presentation pathway is not known, despite the role of $CD4^+$ T cells in coordinating immune responses and in limiting HSV-1 replication and spread.

The protective capacity of the $CD4^+$ T-lymphocyte subset has been described for several model systems. Mice deficient in $CD4^+$ T cells exhibit increased susceptibility to cutaneous HSV-induced lesions, implicating these cells in the control of zosteriform disease (29). Furthermore, MHC class II-mediated immune responses are critical in the protection of mice from ocular or intraperitoneal challenge after vaccination (15, 35). Importantly, $CD4^+$ T cells also act to control HSV infection in the central nervous system and trigeminal ganglia. In the murine model of infection, either $CD4^+$ T or $CD8^+$ T cells alone can clear virus from the trigeminal ganglia, suggesting that both subsets operate to promote the establishment of latency (16), and mice depleted of $CD4^+$ T cells experience more severe infections of the nervous system (37). Furthermore, $CD4^+$ cells are also implicated in limiting latent infection following challenge in a replication-defective vaccination model (35).

A pathogenetic function also ascribed to $CD4^+$ T cells during HSV-1 keratitis is the induction of a bystander inflammatory response and the induction of cytokines in both human and murine infections (14, 38). In humans, virus-reactive $CD4^+$ T cells have been shown to localize to the cornea and are implicated in an immunopathological role in keratitis etiology (24). Also, mononuclear infiltrates in murine models of HSV encephalitis comprise both $CD4^+$ and $CD8^+$ T cells, which have been implicated in immune-mediated pathology (7, 22, 36).

The contribution of $CD4^+$ T cells to the immune control of virus infections and to disease exacerbation can be attributed to the release of cytokines, direct contact with other lymphocytes, or cytotoxic activity. In addition to direct antiviral effects associated with the release of gamma interferon, the release of cytokines is critical to the stimulation of cytotoxic $CD8^+$ T

* Corresponding author. Mailing address: The Marjorie B. Kovler Viral Oncology Laboratories, The University of Chicago, 910 E. 58th St., Chicago, IL 60637. Phone: (773) 702-1898. Fax: (773) 702-1631. E-mail: bernard@cummings.uchicago.edu.

cells, the activation of B cells and the development of virus-specific antibody, and the activation of nonspecific immune cells such as NK and macrophages. Thus, $CD4^+$ T cells play an important role in coordinating and promoting immune responses.

Because $CD4^+$ T cells are believed to exert both protective and pathogenic roles during HSV infections, attenuation or modulation of $CD4^+$ T-cell function may represent an obvious and potentially critical requirement of this highly successful pathogen. Recent studies have shown that HSV-1 can diminish the T-cell stimulatory capacity of dendritic cells, B lymphoblastoid lines, and macrophages (3, 20, 25, 46). However, these studies indicated that HSV-1 does not directly target MHC class II cell surface expression.

We sought to determine whether HSV-1 could interfere with antigen presentation via the MHC class II pathway. The studies were done with U373-MG glioblastoma cells stably transfected with the major MHC class II transcriptional activator (CIITA). This system is relevant in that glial cells, from which the malignant glioblastomas are derived, are a natural MHC class II protein-expressing cell type infected by HSV-1 in vivo (30). U373 cells normally produce low levels of MHC class II, which can be upregulated upon exposure to interferons. U373 lines stably expressing CIITA synthesize levels of MHC class II required for biochemical and fluorescence-activated cell sorter (FACS) analysis and are capable of presenting antigens to $CD4^+$ T cells in vitro (50). Furthermore, unlike many immortalized B-lymphocyte lines used in MHC class II analyses, those used in our studies were not complicated by underlying latent infections with Epstein-Barr virus. We present evidence that HSV-1 can downmodulate MHC class II cell surface expression in glioblastoma cells. Furthermore, HSV-1-infected cells undergo a cellular response resulting in elevated class II surface expression and increased endocytosis, and HSV-1 disables this cellular response through a mechanism dependent on expression of the $\gamma_1$34.5 gene product.

MATERIALS AND METHODS

Cells and viruses. The U373-MG HisCIITA human glioblastoma lines His16 and His28 were described elsewhere (50). The cell lines were maintained in Dulbecco's modified Eagle's medium supplemented with 10% fetal calf serum.

HSV-1(F) is the prototype HSV-1 strain used in this laboratory (11). The following mutant strains were used in these analyses: R3616, which lacks 1 kbp in both copies of the $\gamma_1$34.5 gene (8); R325, which lacks the carboxyl-terminal 200 codons of the ICP22 gene (41); R7041, which lacks codons 69 to 357 of the U_S3 gene (42); R7356, which lacks codons 155 to 412 of the U_L13 gene (43); R2621, in which the *Escherichia coli lacZ* replaced the U_L41 open reading frame encoding the virus host shutoff (*vhs*) protein (40); and R7032, which lacks the gene encoding the U_S8 open reading frame (ORF) (32). Viruses were propagated in HEp-2 or Vero cells obtained from the American Type Tissue Collection and maintained in Dulbecco's modified Eagle's medium supplemented with 10% fetal calf serum (HEp-2) or newborn calf serum (Vero). The titers of the viruses were determined on Vero cells.

Antibodies. The following antibodies were used in these studies: monoclonal antibody DA6.147, which recognizes HLA-DRα chains, and monoclonal antibody PIN.1, which is specific for invariant chain (gifts from P. Cresswell, Yale University); and fluorescein isothiocyanate (FITC)- or phycoerythrin (PE)-conjugated anti-HLA-DR (clone TÜ36), anti-HLA-A, -B, and -C (clone G46-2.6), and anti-CD71 (transferrin receptor, clone M-A712) antibodies, which were purchased from BD PharMingen.

FACS analysis of cell surface proteins and endocytic uptake of fluorescent tracers. Cells grown in 25-cm^2 flasks were exposed to 10 PFU of virus per cell and incubated at 37°C. At the times indicated in Results, cells were dislodged from the plastic surface with versene, chilled to 4°C, rinsed three times with cold phosphate-buffered saline (PBS), fixed in 2% paraformaldehyde, rinsed again three times with cold PBS, reacted with FITC- or PE-conjugated anti-HLA-DR, anti-HLA-A, -B, and -C, or anti-CD71 antibodies according to the manufacturer's recommendations, rinsed again with cold PBS, and analyzed in a FACscan II (Becton-Dickinson). The data were analyzed with the aid of CellQuest (Becton-Dickinson) software. Alternatively, mock- and virus-infected cells were harvested as described above, reacted with antibodies, rinsed in PBS, and analyzed directly or fixed in 2% paraformaldehyde prior to analysis. In double-stain experiments, single-stained controls were used to appropriately adjust fluorochrome compensation levels. Channel FL1 was used for FITC, and FL2 was used for PE. To test the effect of the proteasomal inhibitor MG132 on cell surface class II protein accumulation, the medium from infected cells was replaced at the times indicated in Results with fresh medium or fresh medium supplemented with 5 μM MG132 (BioMol) or 20 μM carboxybenzyl-leucyl-leucyl-leucine vinyl sulfone (Z-L_3-VS; obtained from H. Ploegh, Harvard University) (5). Cells were harvested for FACS analysis as described above. For endocytosis studies, cells grown in 150-cm^2 flasks and exposed to 10 PFU of virus per cell were harvested by trypsin digestion at the times indicated in Results. The dislodged cells were rinsed and resuspended in prewarmed medium containing 1 mg of FITC-conjugated dextran (M_r, 40,000; lysine fixable) per ml or lucifer yellow (potassium salt) (Molecular Probes). Cells were exposed to the fluorescent tracers for 15 or 30 min at 37°C with rotation, rinsed three times with cold PBS containing 2% fetal bovine serum and one time in cold PBS, fixed, and subjected to FACS analysis as described above. The background for each sample was determined by the inclusion of a duplicate maintained at 4°C during the exposure time.

Preparation of cell lysates and immunoblotting. Cells grown in 25-cm^2 flasks were harvested 12 h after exposure to 10 PFU of virus per cell, rinsed with PBS, and fractionated in lysis buffer containing 25 mM Tris, 250 mM NaCl, 5 mM EDTA, 0.1% Triton X-100, and 1% (vol/vol) protease inhibitor cocktail (Sigma). Lysates were rotated at 4°C for 1 h, and nuclei were pelleted by centrifugation. Seventy-five micrograms of protein from the cytoplasmic fractions was subjected to electrophoresis in sodium dodecyl sulfate (SDS)-polyacrylamide gels, transferred to a nitrocellulose sheet, and reacted with antibody DA6.147 and then with horseradish peroxidase-conjugated goat anti-mouse antibody (Sigma). Bound antibodies were visualized by chemiluminescence (ECL, Amersham Pharmacia Biotech UK).

[^{35}S]methionine labeling and immunoprecipitation. Replicate 25-cm^2 flask cultures were radiolabeled with [^{35}S]methionine-cysteine (110 μCi/1 $\times$ 10^6 to 3×10^6 cells) for 2 h immediately before or after exposure to 10 PFU of virus per cell, rinsed extensively with unlabeled media, replaced with unlabeled media, and harvested at the intervals stated in Results. To test the effects of the proteasomal inhibitor MG132, cells were labeled for 2 h immediately after infection, exposed to medium containing 5 μM MG132 at 4 h after infection, and harvested at 2, 4, 8, or 12 h after infection. In all experiments, cell lysates were precleared with 20 μl of rehydrated protein A beads and class II complexes were immunoprecipitated with antibody DA6.147 from pooled replicate cultures disrupted with 1% digitonin lysis buffer as described elsewhere (50). Antigen-antibody complexes were captured with 50 μl of rehydrated protein A beads preincubated with unlabeled lysate from mock-infected cells. During the last rinse, each sample was divided into two aliquots and resuspended in loading buffer containing 2% SDS and 5% β-mercaptoethanol. One aliquot was boiled for 5 min, and the replicate was left at room temperature. Samples were separated by SDS-polyacrylamide gel electrophoresis. Gels were fixed in a mixture of methanol, acetic acid, and water (2:1:7) and dried, and radiolabeled proteins were visualized by autoradiography.

Invariant chain analyses were performed as described elsewhere (50). In brief, cells were pulsed with [^{35}S]methionine-cysteine 2 h prior to infection, and cells were harvested 12 h after infection or in a second experiment at 0 or 12 h after infection. To immunoprecipitate total invariant chain, cells were solubilized in Tris-buffered saline (TBS; 25 mM Tris [pH 7.4], 150 mM NaCl) with 1% SDS and protein complexes were denatured by incubating lysates at 95°C for 10 min. Lysates were diluted 10-fold in TBS containing 1% NP-40 prior to immunoprecipitation with antibody PIN.1. MHC class II-associated invariant chain was analyzed first by disruption of cells in digitonin lysis buffer and immunoprecipitation with antibody DA6.147. MHC class II protein complexes were eluted in TBS containing 1% SDS. Complexes were denatured by heating at 95°C for 10 min, diluted 10-fold in TBS containing 1% NP-40, and reimmunoprecipitated with antibody PIN.1. After electrophoretic separation of immunoprecipitated proteins, the gels were fixed, dried, and visualized by autoradiography or transferred to nitrocellulose prior to visualization by autoradiography. To control for the specificity and efficacy of total and sequential immunoprecipitations, the blots also were probed with DA6.147 or PIN.1 and the bands were visualized by chemiluminescence.

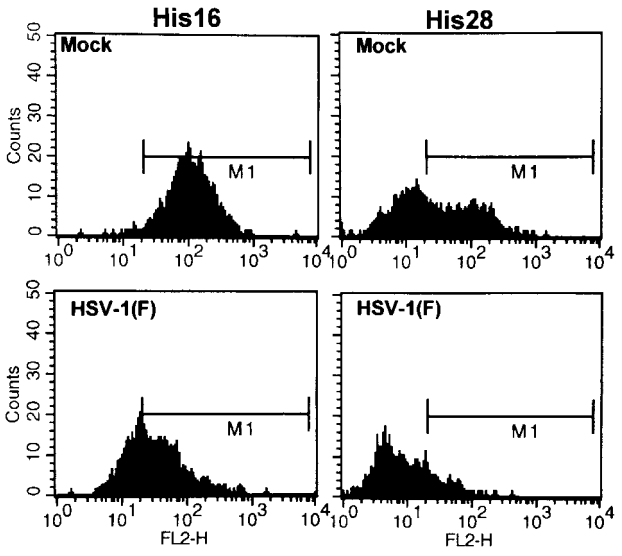

FIG. 1. Histograms of cell surface MHC class II levels in mock- and HSV-1(F)-infected CIITA-transfected U373-MG cells analyzed by FACS. Replicate 25-cm^2 flask cultures were mock infected or exposed to 10 PFU of HSV-1(F) per cell, harvested at 12 or 16 h after infection, fixed in paraformaldehyde, and analyzed for cell surface MHC class II expression by FACS. Histograms are shown for high-level class II-expressing His16 or moderate-level class II-expressing His28 cells at 16 h after infection reacted with PE-conjugated anti-HLA-DR antibody.

RESULTS

Decreased cell surface MHC class II in HSV-1-infected glioblastoma cells. To test whether HSV-1 can interfere with or modulate antigen presentation via the MHC class II pathway, we analyzed the consequences of viral infection of two clones of U373-MG glioblastoma cells stably transfected with CIITA, the major MHC class II transactivator. These were the U373-His28 and U373-His16 cell lines, which express high and moderate levels of MHC class II proteins, respectively. In this series of experiments, replicate cultures of His28 and His16 cells grown in 25-cm^2 flasks were exposed to 10 PFU of virus per cell. At 12 and 16 h after infection, the cells were dislodged from the plates, fixed in paraformaldehyde, and reacted with fluorescently conjugated HLA-DR-specific antibody (clone TÜ36). This antibody reacts with the class IIα chain of class II complexes and does not detect isolated class IIα chains. The percentage of cells expressing cell surface HLA-DR molecules and the mean fluorescence of the cell population in which class II complexes were detected were quantified by FACS analysis.

As shown in Fig. 1 and Table 1, there was a clear shift toward decreased MHC class II surface expression at 12 and 16 h after infection in both cell lines compared to the results for mock-infected cultures. By 12 h after infection, the mean fluorescence in HSV-1(F)-infected cells was approximately twofold lower than those observed in mock-infected cells in both the high- and moderate-level MHC class II-expressing lines. The diminished mean fluorescence also correlated with a decrease in the percentage of cells with detectable MHC class II protein at the cell surface. In the high-level class II-expressing His16 line, the small decrease in the percentage of cells expressing detectable class II observed at 12 h was magnified at 16 h after infection, when 37% fewer cells expressed detectable surface class II protein (Table 1). A similar loss was observed in infected His28 cells. In the second experiment, 19% fewer cells expressed detectable cell surface levels of MHC class II by 13 h after infection in both cell lines.

To test whether the loss of cell surface MHC class II proteins in infected cells was due to enhanced degradation of these proteins by the ubiquitin proteasome-mediated pathway, MHC class II surface levels were measured after treating cells with proteasomal inhibitors. In the next series of experiments, His16 cells and His28 cells were mock infected or exposed to 10 PFU of HSV-1(F) per cell. At 8 h after infection, the medium was replaced with fresh medium or medium containing 5 μM MG132. In a second experiment (His16 only), medium was replaced 6 h after infection with fresh medium or medium supplemented with either 5 μM MG132 or 20 μM Z-L_3-VS. At 12 or 14 h after infection, the cells were harvested, reacted with anti-HLA-DR antibodies, and analyzed by FACS. As shown in Fig. 2 and Table 2, exposure to proteasomal inhibitors did not result in increased accumulation of MHC class II protein at the cell surface. Furthermore, the absence of an effect on the MHC class II surface phenotype could not be ascribed to low permeability of the drug under these conditions, as treatment with Z-L_3-VS has been previously shown to act in U373-MG cells (50).

TABLE 1. Cell surface MHC class II expression in mock- and F-infected glial cells[a]

	Cell line	Virus	12–13 h after infection		16 h after infection	
			% Positive	Mean fluorescence	% Positive	Mean fluorescence
Expt 1	His16	Mock	99	181	99	132
		HSV-1 (F)	91	92	62	60
	His28	Mock	56	130	50	103
		HSV-1(F)	37	59	14	46
Expt 2	His16	Mock	96 ± 0.4	139 ± 9.7	ND	ND
		HSV-1(F)	77 ± 3.0	66 ± 4.0	ND	ND
	His28	Mock	40 ± 2.8	72 ± 4.1	ND	ND
		HSV-1(F)	21 ± 0.8	41 ± 0.7	ND	ND

[a] Cells were reacted with PE-conjugated anti-HLA-DR antibodies and subjected to FACS analyses as described in Materials and Methods. ND, not determined. In experiment 1, replicate 25-cm^2 cultures were harvested, combined, and analyzed at 12 and 16 h after infection. In experiment 2, triplicate 25-cm^2 flasks were harvested at 13 h after infection and standard deviation values are included.

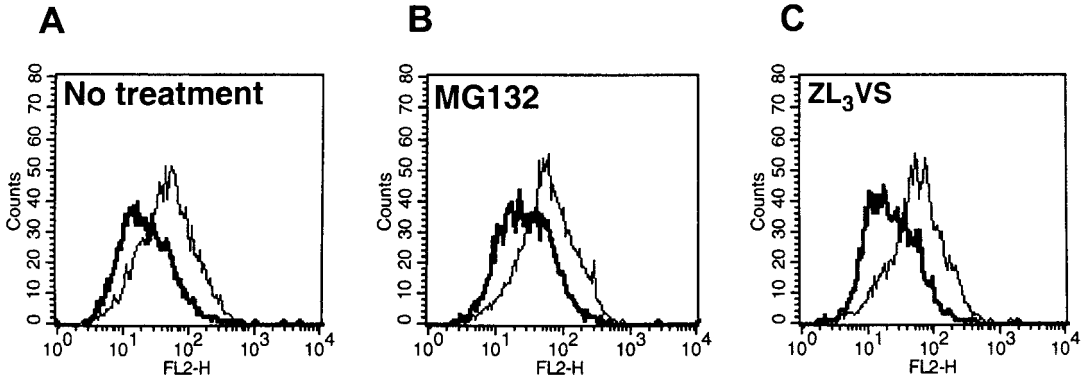

FIG. 2. Histograms of cell surface MHC class II levels in mock- and HSV-1(F)-infected CIITA-transfected U373-MG cells treated with proteasomal inhibitors and analyzed by FACS. Replicate 25-cm^2 flask cultures of His16 cells were mock infected (thin lines) or exposed to 10 PFU of HSV-1(F) per cell (thick lines) and treated with the proteasomal inhibitors MG132 or Z-L_3-VS at 6 h after infection. The cells were harvested at 12 h after infection, fixed in paraformaldehyde, and analyzed for cell surface MHC class II expression by FACS. Histograms are shown for high-level class MHC II-expressing His16 cells reacted with PE-conjugated anti-HLA-DR.

HSV-1 gene products affect MHC class II expression. A possible explanation for the loss of MHC class II molecules on cell surfaces is that the synthesis of these proteins ceases after infection. One potential culprit is the *vhs* protein, the product of the U_L41 ORF. This protein induces a nonspecific degradation of mRNA early in infection. To test this hypothesis, replicate cultures of His16 cells grown in 25-cm^2 flasks were exposed to 10 PFU of HSV-1(F) or R2641 (ΔU_L41) per cell. At 4, 8, and 12 h after infection, the cells were harvested and cell surface class II levels were quantified by FACS analysis as described in Materials and Methods. The results (Fig. 3) were as follows. The mean fluorescence reflecting the presence of MHC class II proteins in HSV-1(F)-infected cells decreased by as early as 8 h (1.3-fold lower than values for mock-infected cells), and surface class II levels continued to fall such that by 12 h, mean fluorescence was approximately 1.6-fold lower than mock values. In contrast, the mean fluorescence of cells exposed to R2641 was approximately 1.5-fold higher than that of mock-infected cells at both 8 and 12 h after infection.

In the second series of experiments, we set out to determine if additional virus gene products could influence cell surface levels of MHC class II. His16 and His28 cells grown in 25-cm^2 flasks were exposed to 10 PFU of wild-type parent HSV-1(F) or the deletion mutants R3616 ($\Delta\gamma_1$34.5), R325 ($\Delta\alpha$22), R7041 (ΔU_S3), or R7356 (ΔU_L13) per cell. The cells were harvested at 14 h after infection and subjected to FACS analysis as described in Materials and Methods. The results (Fig. 4) were as follows.

(i) In both His16 and His28 cell lines, the accumulation of cell surface MHC class II proteins 14 h after infection with wild-type HSV-1(F) decreased by between 50% (His16) and 30% (His28).

(ii) In cells infected with R3616 ($\Delta\gamma_1$34.5 mutant), there was a twofold increase in the amount of cell surface MHC class II proteins compared to that of mock-infected cells and as much as a three- to fourfold increase compared to that of HSV-1(F)-infected cells. The percentage of His28 cells in which MHC class II was detected rose from 46% (mock-infected) to 86% (R3616-infected).

(iii) In cells infected with the R325 ($\Delta\alpha$22), R7041 (ΔU_S3), or R7356 (ΔU_L13) mutants, MHC class II cell surface protein levels were either similar to those of mock-infected cells (ΔU_S3 or ΔU_L13 mutants) or reproducibly slightly elevated ($\Delta\alpha$22 mutant).

TABLE 2. Effect of proteosomal inhibitors on surface class II expression[a]

Cell line	Virus	No treatment		MG132		Z-L_3-VS	
		% Positive	Mean fluorescence	% Positive	Mean fluorescence	% Positive	Mean fluorescence
Expt 1[b]							
His16	Mock	99	264	99	299	ND[d]	ND
	HSV-1(F)	98	137	98	150	ND	ND
His28	Mock	50	139	51	144	ND	ND
	HSV-1(F)	36	88	35	71	ND	ND
Expt 2[c]							
His16	Mock	83	71	89	74	88	80
	HSV-1(F)	46	48	60	54	49	45

[a] Cells were reacted with PE-conjugated anti-HLA-DR antibodies and subjected to FACS analyses as described in Materials and Methods.
[b] Cells were treated with MG132 8 h after infection and harvested for analysis at 12 (His16) or 14 (His28) h after infection.
[c] Cells were treated with MG132 or Z-L_3-VS 6 h postinfection and harvested for analysis 12 h after infection. The lower basal levels of surface class II in experiment 2 reflect the use of higher-passage cells in this experiment.
[d] ND, not determined.

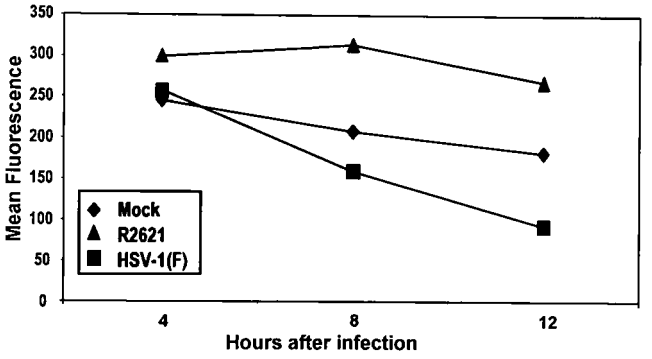

FIG. 3. Effect of the virus host shutoff function on accumulation of cell surface MHC class II levels in infected cells. Replicate 25-cm^2 flask cultures of His16 cells were mock infected (diamonds) or exposed to 10 PFU of HSV-1(F) (squares) or R2621 (triangles) per cell. Cells were harvested at 4, 8, and 12 h after infection, fixed in paraformaldehyde, and analyzed for cell surface MHC class II expression by FACS. Mean fluorescence values are shown for high-level MHC class II-expressing His16 cells reacted with PE-conjugated anti-HLA-DR.

The changes in MHC class II cell surface expression in infected cells could not be attributed to the reaction of antibodies with intracellular antigen. Analyses of unfixed cells yielded the same distribution of MHC class II surface proteins as that obtained on fixed cells reacted with antibody (data not shown). Furthermore, cells infected with a mutant harboring a disruption of the U_S8 gene, which encodes gE, exhibited the same loss of cell surface MHC class II levels as did wild-type-infected cells (data not shown). Thus, the Fc binding properties of gE/gI also are unlikely to account for the elevated cell surface MHC class II levels in R3616 ($\Delta\gamma_1$34.5)- and R2621 (ΔU_L41)-infected cells.

We conclude from these studies that the accumulation of MHC class II proteins on the surface of infected cells is regulated by viral gene products. A central question arising from these results is whether the cell surface MHC class II levels in cells infected with these viruses reflect a change in the total amount of MHC class II protein or a redistribution of the proteins in cellular compartments.

The decrease in MHC class II proteins on the surface of infected cells does not reflect a decrease in the total amounts of the proteins. To test whether the levels of MHC class II proteins at the cell surface reflect changes in the total amounts of class II present in the infected cells, 25-cm^2 flask cultures of His16 cells were mock infected or exposed to 10 PFU of HSV-1(F) parent or deletion mutant virus per cell. The cells were harvested at 12 h after infection, solubilized, subjected to electrophoresis in a denaturing polyacrylamide gel, transferred to a nitrocellulose sheet, and reacted with antibody to DA6.147, which specifically recognizes MHC class IIα chains. The results, shown in Fig. 5, indicate that the amounts of MHC class IIα chains in mock-infected cells were not significantly different from those present in lysates of cells infected with the wild-type or mutant viruses. Analyses of MHC class IIα chain levels in lysates of mock- or virus-infected His28 cells yielded similar results (data not shown). These results indicate that the decrease in the cell surface MHC class II protein was the consequence of redistribution rather than a substantial loss or gain of these proteins.

The increase in MHC class II proteins in cells infected with R3616 ($\Delta\gamma_1$34.5) or R2621 (ΔU_L41) is not due to a general increase in the accumulation of cell surface proteins. One hypothesis that could explain the results obtained with the R3616 and R2641 deletion mutants is that the increased accumulation of MHC class II proteins reflects a general increase in the accumulation of cellular proteins on the cell surface. To test this hypothesis, replicate 25-cm^2 flask cultures of His16 or His28 cells were harvested at 13 h after mock infection or exposure to 10 PFU of wild-type parent or R3616 or R2621 mutant virus per cell. Cells were reacted with antibodies to MHC class II or class I proteins or the transferrin receptor and subjected to FACS analysis. The results for both cell lines (Fig. 6) were as follows.

(i) In mock-infected cells, cell surface MHC class I and II molecules were expected to exhibit similar stability over the time period used in this experiment, and thus, analysis of MHC class I molecules served as a useful control. Cell surface MHC class I levels were diminished in R3616-, R2621-, and HSV-1(F)-infected His28 cells relative to those observed in mock-infected cells. A similar pattern was observed in the His16 cells, with the exception of R2621-infected cells, which exhib-

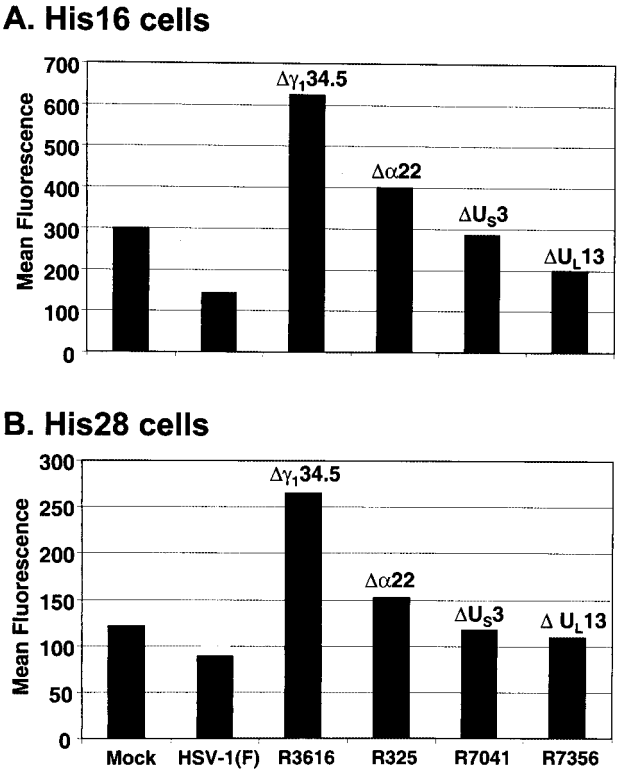

FIG. 4. Effects of various virus gene deletions on accumulation of cell surface MHC class II in infected CIITA-transfected U373-MG cells. Replicate 25-cm^2 flask cultures of His16 (A) or His 28 (B) cells were mock infected or exposed to 10 PFU of the indicated viruses per cell. The genes disrupted in each virus strain are indicated above the bars. At 14 h after infection, cells were harvested, fixed in paraformaldehyde, and analyzed for cell surface MHC class II expression by FACS. MHC class II cell surface mean fluorescence values are shown for cells reacted with PE-conjugated anti-HLA-DR.

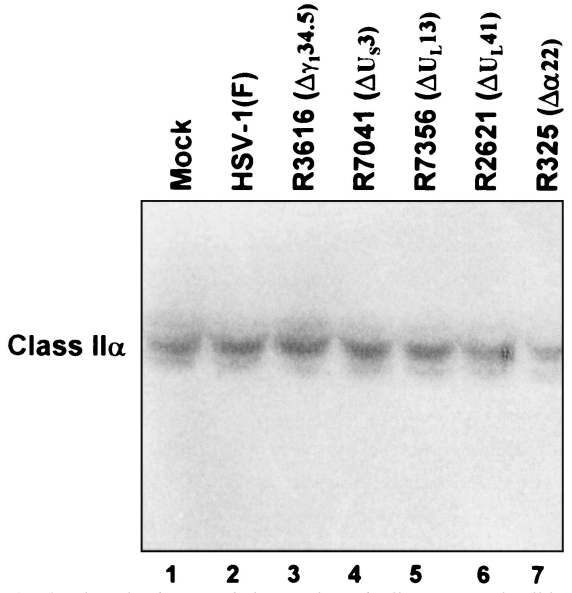

FIG. 5. Phosphorimage of electrophoretically separated cell lysates reacted with antibody recognizing MHC class IIα chains. Replicate 25-cm^2 flask cultures of His16 cells were mock infected or exposed to 10 PFU of the indicated viruses per cell, harvested 12 h after infection, and solubilized. Equivalent amounts of protein from each lysate were electrophoretically separated in a denaturing gel, electrically transferred to a nitrocellulose sheet, and reacted with antibody DA6.147.

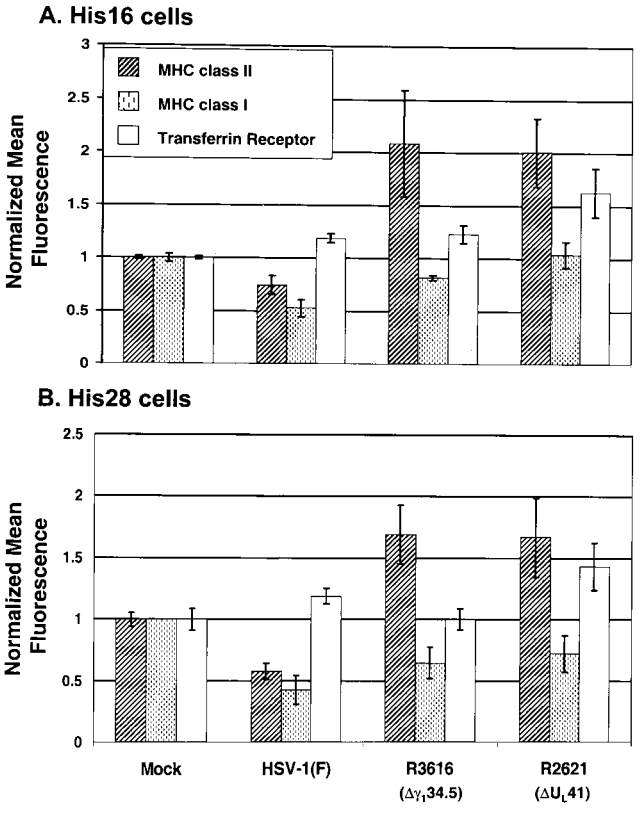

FIG. 6. Effects of various gene deletions on accumulation of cell surface MHC class I and II and transferrin receptor levels in infected CIITA-transfected U373-MG cells. Replicate 25-cm^2 flask cultures of His16 (A) and His 28 (B) cells were mock infected or exposed to 10 PFU of the HSV-1(F), $\Delta\gamma_1$34.5, or ΔU_L41 viruses per cell. In a second experiment, triplicate 25-cm^2 flask cultures were infected as described above. At 13 h after infection, cells were harvested, fixed in paraformaldehyde, reacted with appropriate antibodies, and analyzed by FACS. Cells were reacted with PE-conjugated anti-HLA-DR and FITC-conjugated anti-HLA-A, -B, or -C or PE-conjugated anti-HLA-DR and FITC-conjugated anti-CD71. Cell surface mean fluorescence values for MHC class II (hatched bars), MHC class I (dotted bars), and transferrin receptor (unfilled bars) were normalized to mock levels. Standard deviation values were calculated from four independent samples derived from two experiments for each cell line.

ited MHC class I surface levels comparable to those of mock-infected cells.

(ii) The levels of transferrin receptor detected at the cell surfaces were slightly elevated in most infected cells and were highest in R2621-infected cells. This pattern suggests the possibility that in wild-type-virus-infected cells, there is a turnover of transferrin receptor without replenishment by new biosynthesis due to the activity of the *vhs* protein.

(iii) Compared to those of mock-infected cells, MHC class II cell surface levels were elevated in R3616- and R2621-infected cells but were diminished in wild-type-virus-infected cells.

These results demonstrate that the three cell surface proteins examined in this study exhibited distinct patterns of modulation upon infection. On the basis of these results we conclude the following. First, increased surface levels of MHC class II proteins in cells infected with the R3616 ($\Delta\gamma_1$34.5) mutant do not reflect an overall increase in the accumulation of cell surface proteins in infected cells. Second, *vhs* appears to cause a reduction in the accumulation of MHC class II proteins on infected cell surfaces.

Differential synthesis and maturation of class II complexes in infected cells. In this series of experiments, pulse-chase radiolabeling and immunoprecipitation experiments were performed with an anti-class II DRα antibody, DA6.147. This antibody efficiently precipitates mature, peptide-loaded class II complexes as well as immature class II complexes associated with invariant chain or invariant chain cleavage products. In these experiments, the biosynthesis and maturation of class II complexes were compared among CIITA-transfected U373-MG cells that were mock infected or exposed to 10 PFU of HSV-1(F), R3616 ($\Delta\alpha_1$34.5), or R2621 (ΔU_L41) per cell.

In the first experiment (Fig. 7) the cells were radiolabeled with a [^{35}S]methionine-cysteine mixture for 2 h immediately after infection. After the labeling period, the cells were rinsed extensively with prewarmed unlabeled medium and incubated in unlabeled medium for chase periods of 0, 2, and 6 h. At these times, cells were harvested and solubilized and MHC class II complexes were immunoprecipitated. During the last rinse, antigen-antibody complexes bound to beads were divided into two equal aliquots. One aliquot was boiled for 5 min to disrupt SDS-stable peptide-loaded complexes. Both the boiled and unboiled samples were subjected to electrophoresis in denaturing polyacrylamide gels, and MHC class II complexes and their constituent molecules were visualized by autoradiography. The generation of SDS-stable peptide-loaded complexes was evaluated by comparing boiled and unboiled samples from mock- and virus-infected lysates. The results were as follows.

(i) A general comparison of the MHC class II biosynthetic profiles shown in Fig. 7A (2 h after infection, no chase period)

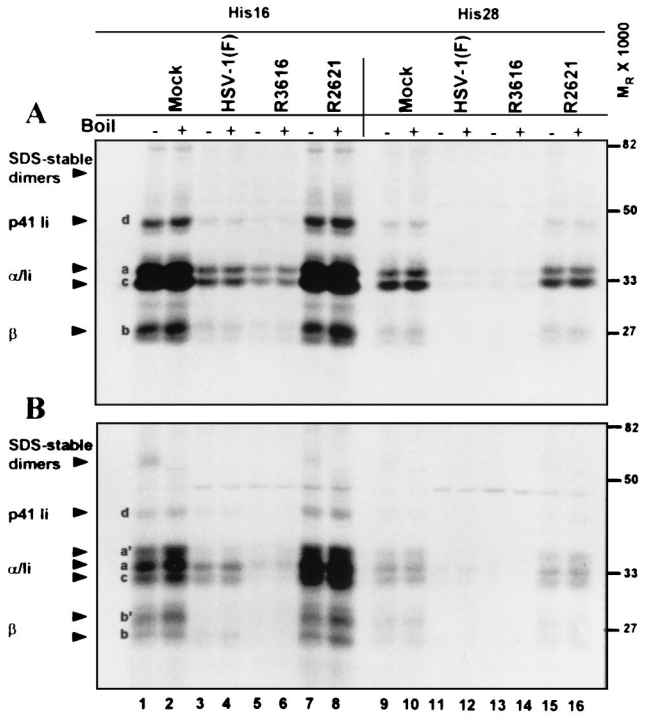

FIG. 7. Autoradiographic image of electrophoretically separated MHC class II complexes immunoprecipitated with antibody DA6.146 from mock- or virus-infected cell lysates. Replicate 25-cm^2 flask cultures of His16 and His28 cells were mock infected or exposed to 10 PFU of the HSV-1(F), $\Delta\gamma_1$34.5, or ΔU_L41 viruses per cell. To radiolabel proteins, cells were incubated in the presence of [^{35}S]methionine for 2 h after infection. Cultures were washed with unlabeled media, and at 2 h (panel A, no chase period), 4 h (2-h chase period, data not shown), or 8 h (panel B, 6-h chase period) after infection, the cells were harvested and solubilized. MHC class II complexes were immunoprecipitated with DA6.147 antibody, separated in 10% denaturing gels, and visualized by autoradiography. Plus and minus signs indicate whether or not samples were boiled. MHC class IIα and -β chains, SDS-stable dimers, and p33 and p41 invariant chain isoforms are indicated on the left with arrowheads. The positions of the molecular weight markers are indicated on the right.

revealed substantial differences in the incorporation of the radiolabeled amino acids into MHC class II complexes in infected cells. In HSV-1(F)-infected cells (lanes 3, 4, 11, and 12), much lower levels of class IIα, class IIβ, and invariant chains were observed compared to those of mock-infected cells (lanes 1, 2, 9, and 10). In R2621-infected cells (lanes 7, 8, 15, and 16), class II protein levels were slightly higher than those observed in mock-infected cells. In R3616-infected cells, the levels of newly synthesized class II complex constituents were similar to (His28) or somewhat lower than (His16) those observed in HSV-1(F)-infected cells. This was consistent, at least in part, with the expression of the *vhs* protein in cells infected with the R3616 ($\Delta\alpha_1$34.5) virus mutant.

(ii) After a 2-h labeling period, class IIα and -β chains in all samples were typical of newly synthesized molecules in the endoplasmic reticulum, with each chain generally appearing as a single band, except the class IIβ chain, which appeared as a doublet (Fig. 7A, no chase, bands a and b). In mock-infected cells at 8 h after infection (Fig. 7B, 6-h chase), modified forms of class IIα and -β and invariant chains appeared (Fig. 7B, lanes 1, 2, 9 and 10, bands a′ and b′). MHC class IIα and -β chain profiles in R2621-infected cells were similar to profiles in mock-infected cells at this time (Fig. 7B, lanes 7, 8, 15, and 16). In cells infected with HSV-1(F), class IIα and -β chains were predominantly in faster-migrating forms than those observed in mock-infected cells (compare lanes 1 and 2 to 3 and 4, bands a versus a′ and b versus b′). Very little monomeric α and β chains of the MHC class II complex were visible at 8 h after infection with the R3616 mutant (lanes 5, 6, 13, and 14).

(iii) At 2 h after infection (Fig. 7A, 0-h chase), stable, peptide-loaded class II complexes had not yet formed in either cell line. By 8 h after infection, the presence of mature α and β chains also correlated with the appearance in mock-infected cells of SDS-stable αβ dimers loaded with peptides. The αβ dimers were disrupted upon boiling (Fig. 7B, lanes 1 and 2). SDS-stable dimers also were observed in R2621-infected cells (Fig. 7B, lane 7). In HSV-1(F)- and R3616-infected cells, the absence of detectable stable dimers could have been related to the general decrease in the amount of radiolabel incorporated into the MHC class II complexes or the generation of peptide-loaded complexes that were not resistant to SDS (Fig. 7B, lanes 3 to 6 and 11). Thus, it was not possible to assess the impact of these infections on class II peptide-loaded dimer formation when using these labeling conditions.

(iv) At 2 h after infection, invariant chain (Ii) isoforms are efficiently immunoprecipitated with class II complexes in mock- and virus-infected cells. In human cells, four Ii isoforms can be synthesized: two are differentiated by alternately spliced forms (p33 and p41), and the other two are differentiated by alternate translation initiation sites (p35 and p43). In mock-infected cells at 8 h after infection, the p33 isoform migrated slightly faster than class IIα chains (Fig. 7B, band c), whereas the p35 isoform and modified p33 isoforms could not be unambiguously differentiated from class IIα chains. The p41 isoform was clearly observed (band d). The amounts of Ii chains correlated with the overall level of radiolabel incorporation in the different infections. The exception to this pattern was the loss of p41 Ii associated with class II complexes at 8 h after infection in R3616-infected cells (compare Fig. 7A, band d, lanes 5 and 6 to Fig. 7B, lanes 5 and 6).

MHC class IIα and -β and Ii chain bands appeared diminished at 8 h compared to those at 2 h after infection in HSV-1(F)- and R3616-infected cells. To test whether the diminished levels of the constituent molecules of the class II complex at 8 h could be attributed to proteasomal degradation, cells were infected and labeled as described above, treated with MG132 at 4 h after infection, and harvested at the times indicated. The results (Fig. 8, 8 h after infection) showed that exposure of cells to MG132 did not change the profiles of accumulated proteins (compare lanes 1 and 2 to 3 and 4, 5 and 6 to 7 and 8, 9 and 10 to 11 and 12, and 13 and 14 to 15 and 16). Therefore, the discrepancy in the levels of monomeric chains between 2 and 8 h after infection shown in Fig. 7 could not be attributed to degradation of class II complexes by a ubiquitin-mediated proteasomal pathway.

Maturation of class II complexes synthesized prior to infection. Maturation of MHC class II protein complexes also was followed in cells pulse-labeled with [^{35}S]methionine for 2 h prior to infection in order to control for the variable levels of class II synthesis after infection. In this experiment, proteins

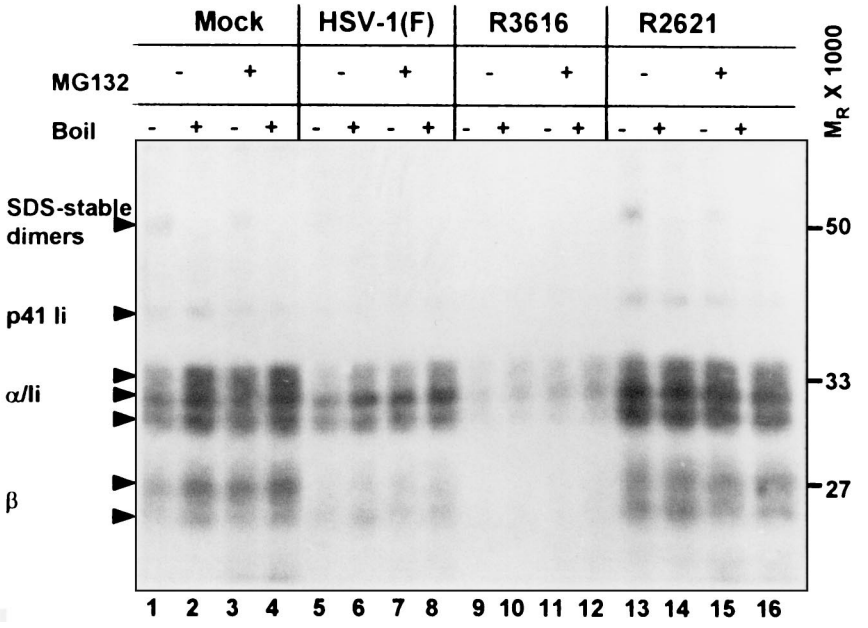

FIG. 8. Autoradiographic image of electrophoretically separated MHC class II complexes immunoprecipitated with antibody DA6.146 from mock- and virus-infected cells treated with the proteasomal inhibitor MG132. Quadruplicate 25-cm^2 flask cultures of His16 cells were mock infected or exposed to 10 PFU per cell of the HSV-1(F), $\Delta\gamma_1$34.5, or ΔU_L41 viruses per cell. To radiolabel proteins, cells were incubated in the presence of [^{35}S]methionine for 2 h after infection. MG132 was administered to one half of the cultures at 4 h after infection. Cells were harvested at 2, 4, 8, or 12 h after infection, and results from the 8-h time point are shown. At each time point, cells were harvested and solubilized and class II complexes were immunoprecipitated with DA6.147 antibody. Proteins were separated in 10% denaturing gels and visualized by autoradiography. Plus and minus signs indicate the presence and absence of MG132 and whether or not samples were boiled. MHC class IIα and -β chains, SDS-stable dimers, and p33 and p41 invariant chain isoforms are indicated on the left with arrowheads. The positions of the molecular weight markers are indicated on the right.

were radiolabeled for 2 h immediately preceding infection. After the labeling period, cells were rinsed extensively with prewarmed unlabeled medium and exposed to 10 PFU of the indicated viruses per cell for 1 h, incubated in unlabeled medium for 8 or 12 h (9- or 13-h chase period, respectively), and processed as described above. The results for His16 (Fig. 9A) and His28 (Fig. 9B) were as follows.

(i) As expected, the overall levels of [^{35}S]methionine incorporation were similar in mock- and virus-infected cells under these conditions. Differences in the amounts of label incorporated between the two cell lines reflect different levels of MHC class II proteins synthesized in the high (His16) and moderate (His28) lines (Fig. 9).

(ii) Peptide-loaded SDS-stable MHC class II dimers appeared in mock-, HSV-1(F)-, R3616-, and R2621-infected cells at both time points (Fig. 9, band a). Because not all peptide-loaded complexes are stable in the presence of SDS, the total levels of peptide-loaded MHC class II dimers could not be compared directly.

(iii) MHC class II complexes still associated with Ii or Ii fragments are sensitive to SDS, and therefore, full-length Ii chain molecules and fragments of Ii should be similar in boiled and unboiled samples. As expected, disruption of peptide-loaded SDS-stable dimers by boiling led to an increase in mature monomeric α and β chains in immunoprecipitations in all samples analyzed (Fig. 9, compare boiled and unboiled lanes, bands b and c). There were two important differences among these virus infections. First, compared to the levels in mock-infected, HSV-(F)-infected, and R2621-infected cell lysates, there was a greater increase in mature monomeric forms of class IIα and -β chains upon boiling, especially at 12 h after infection (lanes 5, 6, 13, and 14, band a), in both His16 and His28 cells infected with R3616. Second, full-length p41 Ii was diminished in MHC class II complexes in R3616-infected lysates, consistent with sequential cleavage of Ii that precedes the loading of complexes with peptide antigens.

Altered invariant chain isoforms associated with class II complexes in infected cells. MHC class II complexes associate with invariant chains in the ER as a nonameric complex (three Ii chains and three αβ dimers) and ultimately localize to an endosomal compartment where Ii is cleaved in a stepwise process prior to the loading of peptide antigens in the binding groove of the MHC class II dimer. The isoforms associated with class II complexes can influence the route of complexes to early endosomes (52) and can potentially influence the activity of proteases in endosomal compartments (4, 12). The results of experiments described earlier in the text suggest that at later times in infection (8 to 12 h), MHC class II protein complexes in R3616-infected lysates exhibited diminished association with full-length p41 Ii compared to those of mock-, HSV-1(F)-, and R2621-infected lysates. To confirm the loss of full-length Ii with MHC class II complexes in R3616-infected cells, total Ii and class II-associated Ii were compared in infected cells pulsed with [^{35}S]methionine for 2 h prior to infection. After the labeling period, cells were rinsed extensively with prewarmed unlabeled medium and cultures were exposed to 10 PFU of the

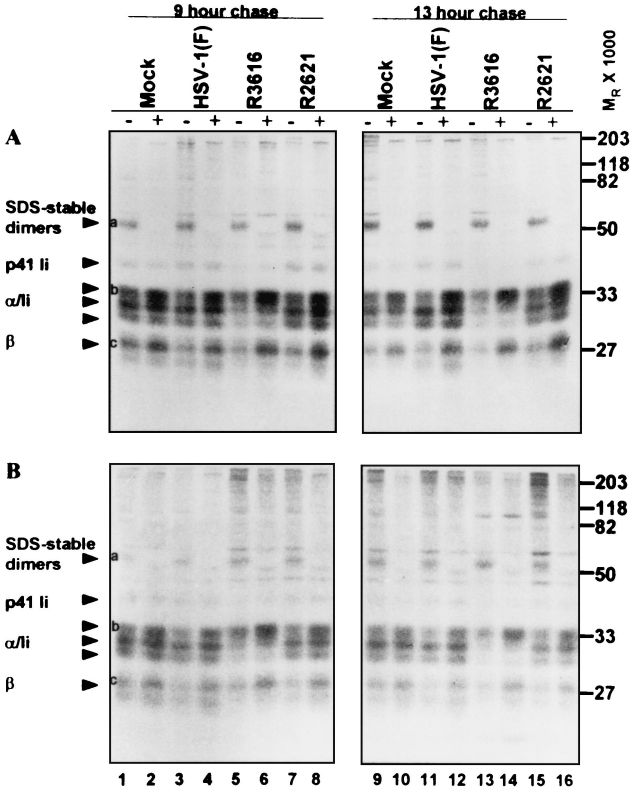

FIG. 9. Autoradiographic image of electrophoretically separated MHC class II complexes synthesized prior to infection and immunoprecipitated with antibody DA6.146 from mock- and virus-infected cells. Replicate 25-cm^2 flask cultures of His16 (A) and His28 (B) cells were incubated in the presence of [^{35}S]methionine for 2 h immediately preceding infection to label cellular proteins. Cultures were washed with unlabeled media and mock infected or exposed to 10 PFU of the HSV-1(F), $\Delta\gamma_1$34.5, or ΔU_L41 viruses per cell. At 8 h (9-h chase period) or 12 h (13-h chase period) after infection, cells were harvested and solubilized and MHC class II complexes were immunoprecipitated with DA6.147. The proteins were separated in 10% denaturing gels and visualized by autoradiography. Plus and minus signs indicate whether or not samples were boiled. MHC class IIα and -β chains, SDS-stable dimers, and p33 and p41 invariant chain isoforms are indicated on the left with arrowheads. The positions of the molecular weight markers are indicated on the right.

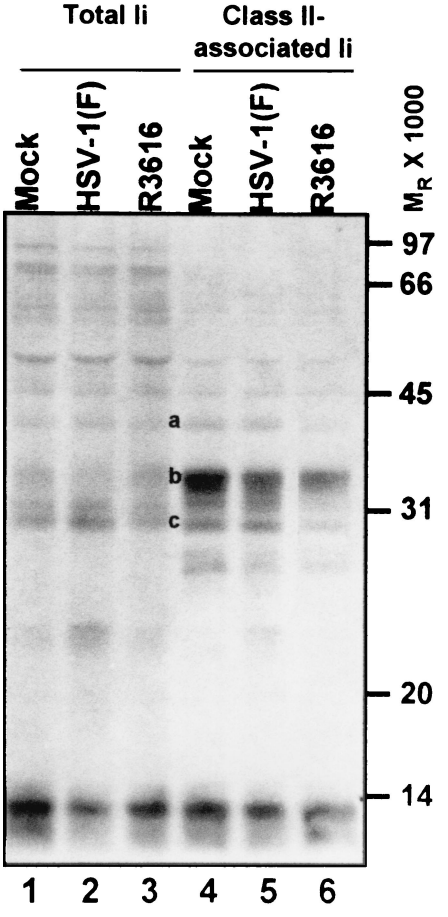

FIG. 10. Autoradiographic image of electrophoretically separated total cellular and MHC class II-associated invariant chain isoforms. Quadruplicate 25-cm^2 flask cultures of His16 cells were incubated in the presence of [^{35}S]methionine for 2 h immediately preceding infection to label cellular proteins. Cultures were rinsed with unlabeled media and mock infected or exposed to 10 PFU of the HSV-1(F), $\Delta\gamma_1$34.5, or ΔU_L41 viruses per cell. At 12 h after infection, cells were harvested and solubilized. Total invariant chain was immunoprecipitated with antibody PIN.1. In replicate samples, MHC class II complexes were immunoprecipitated with antibody DA6.147. Subsequently, MHC class II complexes were isolated and denatured, and samples were subjected to a second immunoprecipitation with antibody PIN.1. The proteins were separated in 10% denaturing gels and visualized by autoradiography. The positions of the molecular weight markers are indicated on the right.

indicated viruses per cell for 1 h and then incubated in unlabeled medium for an additional 12 h. At these times, cells were harvested and solubilized. MHC class II complexes were denatured, and total Ii chains were immunoprecipitated with antibody PIN.1. From replicate samples not subjected to denaturing conditions, class II complexes were immunoprecipitated and denatured and MHC class II-associated Ii were immunoprecipitated with antibody PIN.1.

SDS-polyacrylamide gel electrophoresis analyses of total lysates showed that all samples incorporated equivalent amounts of label (data not shown). The results (Fig. 10) indicated that although the total Ii levels were similar in the various lysates (lanes 1 to 3), lower levels of full-length Ii were associated with class II complexes in R3616-infected lysates than in mock- and HSV-1(F)-infected lysates at 12 h after infection (lane 6 versus lanes 4 and 5; note bands a and c). Rather, recently synthesized MHC class II complexes in lysates from cells infected with the $\gamma_1$34.5 mutant were predominately associated with a band migrating at an M_r of approximately 35,000. This band was most likely the p35 Ii isoform (band b).

From analysis of MHC class II complex biosynthesis and maturation in mock- and HSV-1(F)-infected cells, we conclude the following. (i) MHC class II protein accumulation in HSV-1(F)-infected cells was restricted in a manner independent of the ubiquitin-proteasome pathway but dependent on the *vhs* function encoded by the U_L41 gene product. (ii) There appeared to be a block in processing or transport of class IIα and -β chains synthesized after infection. Finally, (iii) infection did not disrupt the maturation of previously synthesized class II complexes. In contrast to what was found in HSV-1(F)-infected cells, very little monomeric MHC class IIα and -β chains

TABLE 3. Uptake of lucifer yellow in infected cells[a]

Virus	Tracer	Pulse time (min)	% Positive[b]
Mock	LY	15	16.7
HSV-1(F)	LY	15	12.9
R3616	LY	15	33.8
Mock	LY	30	ND[c]
HSV-1(F)	LY	30	19.2
R3616	LY	30	33.5
Mock	None	30	1.5[d]

[a] Cells exposed to LY were fixed and analyzed for fluorescence as described in Materials and Methods.
[b] The percentage of cells positive for LY fluorescence was determined by subtracting the percentage of positive cells pulsed at 4°C from the percentage of positive cells pulsed at 37°C.
[c] ND, not determined.
[d] The percentage of positive cells was only determined after 37°C pulse.

were evident in R3616-infected lysates in which proteins were labeled prior to infection and in which SDS-stable peptide-loaded dimers were not disrupted (unboiled) at 12 h after infection. Monomeric α and β chains became apparent upon disruption of SDS-stable dimers. Also in contrast to HSV-1(F)-infected cells, the amounts of MHC class II-associated full-length invariant chain isoforms were decreased in R3616-infected cells, suggesting that invariant chain was cleaved in this population of class II complexes. One interpretation of these results is that the majority of MHC class II complexes synthesized prior to infection in R3616-infected cells were loaded with peptide by 12 h after infection.

Altered endocytic capacity in infected cells correlates with the class II surface phenotype. MHC class II complexes are typically loaded with exogenously derived peptides derived from antigens captured by endocytosis in antigen-presenting cells. The rate of antigen uptake through endocytosis is controlled in professional antigen-presenting cells. To determine whether the cellular changes observed in cells infected with R3616 included the regulation of endocytic capacity, the uptake of fluorescent tracers was monitored in infected cells. His28 cells in 150-cm^2 flasks were mock infected or exposed to 10 PFU of HSV-1(F) or R3616 per cell, harvested at 13 h after infection, and divided into replicate samples and exposed for 15 or 30 min at 37°C to untreated medium or medium containing the fluorescent tracers lucifer yellow or FITC-dextran. At the end of the exposure interval the cells were rinsed and analyzed by FACS. Lucifer yellow is a hydrophilic dye taken up exclusively through macropinocytosis (fluid-phase endocytosis) in dendritic cells. FITC-conjugated dextran is taken up predominantly through macropinocytosis but can also enter cells through receptor-mediated endocytosis by binding the mannose receptor (47).

As shown in Tables 3 and 4, at 13 h after infection the uptake of both tracers was diminished in HSV-1(F)-infected cells compared to that in mock-infected cells. Because low levels of lucifer yellow were measured, uptake was evaluated according to the percentage of cells exhibiting positive fluorescence (Table 3). Uptake and quantification of FITC-dextran were efficient, with 86 to 88% of cells exhibiting positive fluorescence after a 30-min exposure interval, and thus, mean fluorescence values were compared for this tracer (Table 4). Interestingly, endocytosis of these tracers was elevated in cells infected with the $\gamma_1$34.5 mutant. In these cells, the mean fluorescence of endocytosed FITC-dextran was almost threefold greater than that of mock-infected cells and fourfold greater than that of HSV-1(F)-infected cells after the 30-min pulse. These results show that virus infection altered the capture of antigens through endocytic pathways in a manner that correlated with changes in cell surface MHC class II levels in glioblastoma cells infected with wild-type and $\gamma_1$34.5 mutant viruses.

DISCUSSION

Suppression of cell-mediated immune responses appears to be critical for viral pathogens which establish latent infections. For the members of the *Herpesviridae* family of viruses, this is underscored by the number and diversity of mechanisms which have evolved to counteract MHC class I-mediated immune responses. Strategies to evade or disrupt MHC class II-mediated T-cell responses also have been reported for HSV-1 (27), varicella-zoster virus (1), Epstein-Barr virus (21, 48), and human herpesvirus 8 (10) but have been most thoroughly characterized for the cytomegaloviruses. Human cytomegalovirus protein US2 mediates degradation of HLA-DRα and HLA-DMα chains, leading to inhibition of antigen-presenting cell function (50). Human and murine cytomegaloviruses also disrupt signaling pathways that interfere with the transcription of MHC class II molecules (18, 34), and infection with murine cytomegalovirus results in downmodulation of class II expression through the induction of interleukin 10 (44). In addition, infection of dendritic cells by murine cytomegalovirus disturbs endocytic and antigen-presenting cell functions (2). The extent to which HSV may modulate MHC class II-mediated antigen-presenting cell functions was not known. In the studies presented in this report, we analyzed the status of MHC class II components in U373-MG glioblastoma cells stably transfected

TABLE 4. Uptake of FITC-dextran in infected cells[a]

Virus	Tracer	Pulse time (min)	% Positive at 37°C	Mean fluorescence 4°C	Mean fluorescence 37°C
Mock	FITC-dextran	15	74	91	88
HSV-1(F)	FITC-dextran	15	78	46	63
R3616	FITC-dextran	15	82	58	230
Mock	FITC-dextran	30	86	42	106
HSV-1(F)	FITC-dextran	30	86	48	74
R3616	FITC-dextran	30	88	46	294

[a] Cells exposed to FITC-dextran were fixed and analyzed for fluorescence as described in Materials and Methods.

with CIITA and infected with wild-type or mutant HSV-1. We report the following findings.

(i) MHC class II protein synthesis was shut off in wild-type-virus-infected cells compared to those in mock-infected cells or cells infected with the ΔU_L41 mutant. A similar or even more pronounced shutoff of synthesis of MHC class II proteins was observed in cells infected with the $\Delta\gamma_1 34.5$ mutant.

(ii) While the total amounts of MHC class II proteins were relatively similar in mock-infected cells and cells infected with the wild-type and mutant viruses, there was a drastic decrease in the accumulation of cell surface MHC class II proteins in wild-type-virus-infected cells. In contrast, there was an increase in the accumulation of MHC class II proteins on the surface of cells infected with the ΔU_L41 mutant and especially on the surface of cells infected with the $\Delta\gamma_1 34.5$ mutant.

(iii) Endocytosis of two marker compounds, lucifer yellow and FITC-conjugated dextran, was significantly increased in cells infected with the $\Delta\gamma_1 34.5$ mutant and reduced in wild-type-virus-infected cells relative to that observed in mock-infected cells.

(iv) In wild-type-virus-infected cells, MHC class II protein complexes synthesized after infection appeared to be blocked in processing or transport. MHC class II protein complexes synthesized prior to infection in R3616-infected cells exhibited a strikingly different profile at 12 h after infection compared to those of wild-type- and R2621-infected cells. Specifically, a large increase in monomeric MHC class IIα and -β chains was observed upon disruption of SDS-stable dimers, and there was a relative loss of full-length invariant chain isoforms. One possibility to account for these findings that is consistent with the increase in cell surface MHC proteins is that the majority of MHC class II complexes synthesized prior to infection are in peptide-loaded form in lysates of $\Delta\gamma_1 34.5$-infected cells.

We conclude from these studies the following. Cells infected with wild-type virus attempt to stimulate the MHC class II response by at least enhancing the transport of MHC class II complexes to the cell surface and increasing endocytosis. These cellular responses are blocked as a consequence of the expression of at least two viral genes, U_L41 and $\gamma_1 34.5$. *vhs*, the product of the U_L41 gene, acts early in infection to block the de novo synthesis of MHC class II proteins. ICP34.5, the product of the $\gamma_1 34.5$ gene, enables the synthesis of one or more viral products made late in infection. The net effects of the function of *vhs* protein and of ICP34.5 is the inhibition of accumulation of MHC class II proteins on the cell surface. Related to these conclusions are the following considerations.

(i) *vhs* protein causes nonspecific degradation of mRNA accumulating during the early stages of infection (reviewed in reference 45). This effect largely disappears at late stages of infection. Therefore, *vhs* protein may act to limit the ability of the cells to respond to infection by destroying cellular transcripts upregulated at early stages of infection. In addition, there is a slight increase in the accumulation of MHC class II proteins during the first 8 h after infection with the R2621 mutant compared with those after the wild-type and mock infections, possibly due to the response of infected cells to viral gene products. One possibility is that increased synthesis of MHC class II proteins during the early hours after infection with the ΔU_L41 virus contributes to the increase in cell surface MHC class II levels. In essence, the observed phenotype of ΔU_L41 virus is consonant with the known functions of *vhs* protein.

(ii) The phenotype of the $\Delta\gamma_1 34.5$ virus-infected cells described in this report is not predicted by the known functions of ICP34.5. The major manifestation of the $\Delta\gamma_1 34.5$ mutant is the shutoff of protein synthesis as a consequence of phosphorylation of the α subunit of the translation initiation factor 2 (eIF-2α) (9, 17). This event is dependent on the initiation of viral DNA synthesis and extrapolates to approximately 5 h after infection. However, the rather dramatic decrease in the synthesis of MHC class II proteins during the first 2 h after infection may also be due to the phosphorylation of eIF-2α. Thus, in the absence of ICP34.5, the phosphorylation of eIF-2α dramatically decreases the synthesis of late (γ) viral proteins. The consequence of this reduction in the accumulation of γ proteins may be twofold. First, it may account for the failure of the mutant to preclude the accumulation of MHC class II complexes at the surface of the infected cell and the increase in endocytosis characteristic of $\Delta\gamma_1 34.5$ mutant infection. Second, the absence or delay in the synthesis of αTIF (VP16) may prolong the interval of time during which the *vhs* protein brought into the cell during infection is effective in degrading mRNA. In cells infected with wild-type virus, newly synthesized αTIF binds to the *vhs* protein and blocks further degradation of mRNA (26).

In cells infected with the $\Delta\gamma_1 34.5$ mutant virus, the total amount of MHC class II proteins was not altered substantially compared to those of wild-type- or mock-infected cells, yet there was considerably more MHC class II at the cell surface. It is likely that in cells infected with the $\Delta\gamma_1 34.5$ virus, there is increased transport of MHC class II complexes from cytoplasmic pools to the cell surface. This increase may be a consequence of increased exocytosis of class II proteins from peptide-loading compartments or other post-Golgi compartments. Endocytosis of specific fluorescent tracers also was increased in R3616-infected cells. This raises the question as to whether endocytosis of MHC class II molecules is similarly elevated in cells infected with the $\Delta\gamma_1 34.5$ mutant virus. One working model to account for these observations is that both increased transport of intracellular pools to the cell surface and enhanced endocytosis and recycling contribute to a net increase in the accumulation of MHC class II molecules on the cell surface. Wild-type HSV-1 appears to block these processes, possibly by expression of unidentified late gene products and through destruction of cellular mRNAs by *vhs* protein.

The accumulation of cell surface MHC class II proteins also may be affected by intracellular regulatory events. In support of this hypothesis, radiolabel pulse-chase and immunoprecipitation experiments suggest differential processing or transport of MHC class II and invariant chain proteins in wild-type-infected cells compared to those in $\Delta\gamma_1 34.5$ mutant-infected cells.

In some respects, the response of glioblastoma cells to infection with the $\Delta\gamma_1 34.5$ mutant resembles the activation of mature dendritic cells (33). For example, cell surface MHC class II protein levels increase in dendritic cells in response to specific activating agents (6). The professional antigen-presenting dendritic cells migrate from peripheral tissues to secondary lymphoid organs. Endocytosis is turned off during migration to ensure that antigens captured in the periphery are

efficiently presented in the secondary lymphoid compartments (47). In contrast, the results presented in this report suggest that glioblastoma cells may exhibit enhanced endocytosis in the absence of viral inhibitory factors that are lacking in $\Delta\gamma_1$34.5 mutant-infected cells. As glial cells do not migrate to lymphoid tissues, the increased endocytic capacity would serve to concentrate antigen in activated glial cells, which in turn would promote efficient antigen presentation in neuronal tissue. Similarly, the block in endocytosis observed in wild-type-infected cells would limit peptide loading and presentation of MHC class II proteins. Diminished endocytic function also has been described in cells infected with pseudorabies virus (49). However, endocytosis of transferrin is unaffected in HSV-1(F)-infected epithelial cells (31). Although this may reflect cell-specific modulation of the endocytic machinery by HSV-1, another possibility is that HSV-1 specifically disrupts fluid-phase uptake (macropinocytosis) but not receptor-mediated endocytosis.

The consequences of viral infections with the mutants described in this report on the stimulation of $CD4^+$ T-cell responses remain to be investigated. Earlier studies have shown that immunostimulatory capacity is diminished in dendritic cells, B-lymphoblastoid lines, and macrophages infected with wild-type HSV-1 (3, 20, 25, 46). However, the significance of infections in these cell types is not clear, as they do not represent the primary target cells of HSV-1 in human infections.

The results presented here demonstrate a previously unknown series of cellular changes that constitute a novel response to infection in glioblastoma cells. Characterization of the factors that trigger or suppress the activation of glioblastoma cells may significantly advance our understanding of HSV infections of the nervous system, the development of therapeutic approaches for HSV infections, especially HSV encephalitis, and the appropriate utilization of HSV for gene delivery or for tumor therapy.

ACKNOWLEDGMENTS

We thank Beatrice Fineschi for invaluable advice.

These studies were aided by grants from the National Cancer Institute (CA87661, CA83939, CA71933, CA78766, and CA88860) to the University of Chicago (B. Roizman) and from the National Eye Institute (EY11245) and National Cancer Institute (CA73996) to the OHSU (D. Johnson).

REFERENCES

1. **Abendroth, A., B. Slobedman, E. Lee, E. Mellins, M. Wallace, and A. M. Arvin.** 2000. Modulation of major histocompatibility class II protein expression by varicella-zoster virus. J. Virol. **74:**1900–1907.
2. **Andrews, D. M., C. E. Andoniou, F. Granucci, P. Ricciardi-Castagnoli, and M. A. Degli-Esposti.** 2001. Infection of dendritic cells by murine cytomegalovirus induces functional paralysis. Nat. Immunol. **2:**1077–1084.
3. **Barcy, S., and L. Corey.** 2001. Herpes simplex inhibits the capacity of lymphoblastoid B cell lines to stimulate $CD4^+$ T cells. J. Immunol. **166:**6242–6249.
4. **Bevec, T., V. Stoka, G. Pungercic, I. Dolenc, and V. Turk.** 1996. Major histocompatibility complex class II-associated p41 invariant chain fragment is a strong inhibitor of lysosomal cathepsin L. J. Exp. Med. **183:**1331–1338.
5. **Bogyo, M., J. S. McMaster, M. Gaczynska, D. Tortorella, A. L. Goldberg, and H. Ploegh.** 1997. Covalent modification of the active site threonine of proteasomal beta subunits and the Escherichia coli homolog HslV by a new class of inhibitors. Proc. Natl. Acad. Sci. USA **94:**6629–6634.
6. **Cella, M., A. Engering, V. Pinet, J. Pieters, and A. Lanzavecchia.** 1997. Inflammatory stimuli induce accumulation of MHC class II complexes on dendritic cells. Nature **388:**782–787.
7. **Chan, W. L., T. Javanovic, and M. L. Lukic.** 1989. Infiltration of immune T cells in the brain of mice with herpes simplex virus-induced encephalitis. J. Neuroimmunol. **23:**195–201.
8. **Chou, J., E. R. Kern, R. J. Whitley, and B. Roizman.** 1990. Mapping of herpes simplex virus-1 neurovirulence to gamma 134.5, a gene nonessential for growth in culture. Science **250:**1262–1266.
9. **Chou, J., and B. Roizman.** 1992. The gamma 1(34.5) gene of herpes simplex virus 1 precludes neuroblastoma cells from triggering total shutoff of protein synthesis characteristic of programmed cell death in neuronal cells. Proc. Natl. Acad. Sci. USA **89:**3266–3270.
10. **Coscoy, L., and D. Ganem.** 2001. A viral protein that selectively downregulates ICAM-1 and B7-2 and modulates T cell costimulation. J. Clin. Investig. **107:**1599–1606.
11. **Ejercito, P., E. D. Kieff, and B. Roizman.** 1968. Characterization of herpes simplex virus strains differing in their effects on social behavior of infected cells. J. Gen. Virol. **2:**357–364.
12. **Fineschi, B., K. Sakaguchi, E. Appella, and J. Miller.** 1996. The proteolytic environment involved in MHC class II-restricted antigen presentation can be modulated by the p41 form of invariant chain. J. Immunol. **157:**3211–3215.
13. **Fruh, K., K. Ahn, H. Djaballah, P. Sempe, P. M. van Endert, R. Tampe, P. A. Peterson, and Y. Yang.** 1995. A viral inhibitor of peptide transporters for antigen presentation. Nature **375:**415–418.
14. **Gangappa, S., S. P. Deshpande, and B. T. Rouse.** 1999. Bystander activation of $CD4^+$ T cells can represent an exclusive means of immunopathology in a virus infection. Eur. J. Immunol. **29:**3674–3682.
15. **Ghiasi, H., D. C. Roopenian, S. Slanina, S. Cai, A. B. Nesburn, and S. L. Wechsler.** 1997. The importance of MHC-I and MHC-II responses in vaccine efficacy against lethal herpes simplex virus type 1 challenge. Immunology **91:**430–435.
16. **Ghiasi, H., G. Perng, A. B. Nesburn, and S. L. Wechsler.** 1999. Either a CD4(+) or CD8(+) T cell function is sufficient for clearance of infectious virus from trigeminal ganglia and establishment of herpes simplex virus type 1 latency in mice. Microb. Pathog. **27:**387–394.
17. **He, B., M. Gross, and B. Roizman.** 1997. The gamma(1)34.5 protein of herpes simplex virus 1 complexes with protein phosphatase 1alpha to dephosphorylate the alpha subunit of the eukaryotic translation initiation factor 2 and preclude the shutoff of protein synthesis by double-stranded RNA-activated protein kinase. Proc. Natl. Acad. Sci. USA **94:**843–848.
18. **Heise, M. T., M. Connick, and H. W. Virgin IV.** 1998. Murine cytomegalovirus inhibits interferon gamma-induced antigen presentation to CD4 T cells by macrophages via regulation of expression of major histocompatibility complex class II-associated genes. J. Exp. Med. **187:**1037–1046.
19. **Hill, A., P. Jugovic, I. York, G. Russ, J. Bennink, J. Yewdell, H. Ploegh, and D. Johnson.** 1995. Herpes simplex virus turns off the TAP to evade host immunity. Nature **375:**411–415.
20. **Hoves, S., H. H. Niller, S. W. Krause, R. Straub, T. Gluck, J. D. Mountz, J. Scholmerich, and M. Fleck.** 2001. Decreased T cell stimulatory capacity of monocyte-derived human macrophages following herpes simplex virus type 1 infection. Scand. J. Immunol. **54:**93–99.
21. **Hsu, D. H., R. de Waal Malefyt, D. F. Fiorentino, M. N. Dang, P. Vieira, J. de Vries, H. Spits, T. R. Mosmann, and K. W. Moore.** 1990. Expression of interleukin-10 activity by Epstein-Barr virus protein BCRF1. Science **250:**830–832.
22. **Hudson, S. J., and J. W. Streilein.** 1994. Functional cytotoxic T cells are associated with focal lesions in the brains of SJL mice with experimental herpes simplex encephalitis. J. Immunol. **152:**5540–5547.
23. **Johnson, D. C., and A. B. Hill.** 1998. Herpesvirus evasion of the immune system. Curr. Top. Microbiol. Immunol. **232:**149–177.
24. **Koelle, D. M., S. N. Reymond, H. Chen, W. W. Kwok, C. McClurkan, T. Gyaltsong, E. W. Petersdorf, W. Rotkis, A. R. Talley, and D. A. Harrison.** 2000. Tegument-specific, virus-reactive CD4 T cells localize to the cornea in herpes simplex virus interstitial keratitis in humans. J. Virol. **74:**10930–10938.
25. **Kruse, M., O. Rosorius, F. Kratzer, G. Stelz, C. Kuhnt, G. Schuler, J. Hauber, and A. Steinkasserer.** 2000. Mature dendritic cells infected with herpes simplex virus type 1 exhibit inhibited T-cell stimulatory capacity. J. Virol. **74:**7127–7136.
26. **Lam, Q., C. A. Smibert, K. E. Koop, C. Lavery, J. P. Capone, S. P. Weinheimer, and J. R. Smiley.** 1996. Herpes simplex virus VP16 rescues viral mRNA from destruction by the virion host shutoff function. EMBO J. **15:**2575–2581.
27. **Lewandowski, G. A., D. Lo, and F. E. Bloom.** 1993. Interference with major histocompatibility complex class II-restricted antigen presentation in the brain by herpes simplex virus type 1: a possible mechanism of evasion of the immune response. Proc. Natl. Acad. Sci. USA **90:**2005–2009.
28. **Lubinski, J., T. Nagashunmugam, and H. M. Friedman.** 1998. Viral interference with antibody and complement. Semin. Cell. Dev. Biol. **9:**329–337.
29. **Manickan, E., and B. T. Rouse.** 1995. Roles of different T-cell subsets in control of herpes simplex virus infection determined by using T-cell-deficient mouse models. J. Virol. **69:**8178–8179.
30. **Markovitz, N. S., D. Baunoch, and B. Roizman.** 1997. The range and distribution of murine central nervous system cells infected with the $\gamma_1$34.5$^-$ mutant of herpes simplex virus 1. J. Virol. **71:**5560–5569.
31. **McMillan, T. N., and D. C. Johnson.** 2001. Cytoplasmic domain of herpes simplex virus gE causes accumulation in the trans-Golgi network, a site of

virus envelopment and sorting of virions to cell junctions. J. Virol. **75:**1928–1940.
32. **Meignier, B., R. Longnecker, P. Mavromara-Nazos, A. E. Sears, and B. Roizman.** 1998. Virulence of and establishment of latency by genetically engineered deletion mutants of herpes simplex virus 1. Virology **162:**251–254.
33. **Mellman, I., and R. M. Steinman.** 2001. Dendritic cells: specialized and regulated antigen processing machines. Cell **106:**255–258.
34. **Miller, D. M., B. M. Rahill, J. M. Boss, M. D. Lairmore, J. E. Durbin, J. W. Waldman, and D. D. Sedmak.** 1998. Human cytomegalovirus inhibits major histocompatibility complex class II expression by disruption of the Jak/Stat pathway. J. Exp. Med. **187:**675–683.
35. **Morrison, L. A., and D. M. Knipe.** 1997. Contributions of antibody and T cell subsets to protection elicited by immunization with a replication-defective mutant of herpes simplex virus type 1. Virology **239:**315–326.
36. **Nakajima, H., M. Kobayashi, R. B. Pollard, and F. Suzuki.** 2000. A pathogenic role of Th2 responses on the severity of encephalomyelitis induced in mice by herpes simplex virus type 2 infection. J. Neuroimmunol. **110:**106–113.
37. **Nash, A. A., A. Jayasuriya, J. Phelan, S. P. Cobbold, H. Waldmann, and T. Prospero.** 1987. Different roles for L3T4+ and Lyt 2+ T cell subsets in the control of an acute herpes simplex virus infection of the skin and nervous system. J. Gen. Virol. **68:**825–833.
38. **Newell, C. K., S. Martin, D. Sendele, C. M. Mercadal, and B. T. Rouse.** 1989. Herpes simplex virus-induced stromal keratitis: role of T-lymphocyte subsets in immunopathology. J. Virol. **63:**769–775.
39. **Ploegh, H. L.** 1998. Viral strategies of immune evasion. Science **280:**248–253.
40. **Poon, A. P., and B. Roizman.** 1997. Differentiation of the shutoff of protein synthesis by virion host shutoff and mutant gamma (1)34.5 genes of herpes simplex virus 1. Virology **229:**98–105.
41. **Post, L. E., and B. Roizman.** 1981. A generalized technique for deletion of specific genes in large genomes: alpha gene 22 of herpes simplex virus 1 is not essential for growth. Cell **25:**227–232.
42. **Purves, F. C., R. M. Longnecker, D. P. Leader, and B. Roizman.** 1987. Herpes simplex virus 1 protein kinase is encoded by open reading frame US3 which is not essential for virus growth in cell culture. J. Virol. **61:**2896–2901.
43. **Purves, F. C., W. O. Ogle, and B. Roizman.** 1993. Processing of herpes simplex virus regulatory protein α22 mediated by the UL13 protein kinase determines the accumulation of a subset of α and γ mRNAs and proteins in infected cells. Proc. Natl. Acad. Sci. USA **90:**6701–6705.
44. **Redpath, S., A. Angulo, N. R. Gascoigne, and P. Ghazal.** 1999. Murine cytomegalovirus infection down-regulates MHC class II expression on macrophages by induction of IL-10. J. Immunol. **162:**6701–6707.
45. **Roizman, B., and D. M. Knipe.** 2001. The replication of herpes simplex viruses, p. 2399–2459. *In* D. M. Knipe, P. M. Howley, M. S. Hirsch, T. P. Monath, and B. Roizman (ed.), Fields virology, 4th ed. Lippincott-Raven Press, Philadelphia, Pa.
46. **Salio, M., M. Cella, M. Suter, and A. Lanzavecchia.** 1999. Inhibition of dendritic cell maturation by herpes simplex virus. Eur. J. Immunol. **29:**3245–3253.
47. **Sallusto, F., M. Cella, C. Danieli, and A. Lanzavecchia.** 1995. Dendritic cells use macropinocytosis and the mannose receptor to concentrate macromolecules in the major histocompatibility complex class II compartment: downregulation by cytokines and bacterial products. J. Exp. Med. **182:**389–400.
48. **Spriggs, M. K., R. J. Armitage, M. R. Comeau, L. Strockbine, T. Farrah, B. Macduff, D. Ulrich, M. R. Alderson, J. Mullberg, and J. I. Cohen.** 1996. The extracellular domain of the Epstein-Barr virus BZLF2 protein binds the HLA-DR beta chain and inhibits antigen presentation. J. Virol. **70:**5557–5563.
49. **Tirabassi, R. S., and L. W. Enquist.** 1998. Role of envelope protein gE endocytosis in the pseudorabies virus life cycle. J. Virol. **72:**4571–4579.
50. **Tomazin, R., J. Boname, N. R. Hegde, D. M. Lewinsohn, Y. Altschuler, T. R. Jones, P. Cresswell, J. A. Nelson, S. R. Riddell, and D. C. Johnson.** 1999. Cytomegalovirus US2 destroys two components of the MHC class II pathway, preventing recognition by CD4+ T cells. Nat. Med. **5:**1039–1043.
51. **Ward, P. L., and B. Roizman.** 1998. Evasion and obstruction: the central strategy of the interaction of human herpesviruses with host defenses, p. 1–32. *In* P. G. Medveczky, H. Friedman, and M. Bendinelli (ed.), Herpesviruses and immunity. Plenum Press, New York, N.Y.
52. **Warmerdam, P. A., E. O. Long, and P. A. Roche.** 1996. Isoforms of the invariant chain regulate transport of MHC class II molecules to antigen processing compartments. J. Cell Biol. **133:**281–291.
53. **York, I. A., C. Roop, D. W. Andrews, S. R. Riddell, F. L. Graham, and D. C. Johnson.** 1994. A cytosolic herpes simplex virus protein inhibits antigen presentation to $CD8^+$ T lymphocytes. Cell **77:**525–535.